

FATIGUE LIFE OF SPECIMENS AFTER WEAR-RESISTANT, MANUFACTURING AND REPAIR SURFACING

I.O. Ryabtsev¹, V.V. Knysh¹, A.A. Babinets¹, S.O. Solovej¹ and V.M. Demenkov²

¹E.O. Paton Electric Welding Institute of the NAS of Ukraine

11 Kazymyr Malevych Str., 03150, Kyiv, Ukraine. E-mail: office@paton.kiev.ua

²State Company «State Scientific and Technical Center for Nuclear and Radiation Safety»

35–37 Vasyl Stus Str., 03142, Kyiv, Ukraine. E-mail: vm_demenkov@sstc.com.ua

Cyclic fatigue life of specimens surfaced by flux-cored wire PP-Np-25Kh5FMS that provides a deposited metal of the type of tool semi-heat-resistant steel was studied. Design of the deposited specimens and procedure of their testing simulated the operating conditions of mill rolls, for surfacing of which flux-cored wire PP-Np-25Kh5FMS is widely used. Cyclic fatigue life of the specimens directly after surfacing, as well as the effectiveness of application of repair surfacing were evaluated to increase the residual cyclic fatigue life of the specimens, in which preliminary testing revealed fatigue cracks in the deposited wear-resistant layer. The numerical method was used to determine the stress-strain state and calculate the stress intensity factor on the front of a nonthrough corner fatigue crack that propagated in a specimen of 40Kh steel with a wear-resistant deposited layer at a three-point zero-to-load cyclic loading. It is shown that the maximum values of the stress intensity factor along the crack front are located at approximately 1 mm distance from the vertical side face in the deepest point of the crack front and during fracture they reach the value of 52–64 MPa $\sqrt{\text{m}}$. During investigations it was shown that application of repair surfacing to the products with fatigue cracks after their long-term service does not result in a significant extension of their cyclic fatigue life after repair. This is related to the fact that after long-term service the defect-free layer of the deposited metal has a considerable level of accumulated fatigue damages. That is why performance of repair of the product region damaged by a fatigue crack, is not effective without a complete removal of the deposited metal layer. The results obtained in this work will be further used as base ones during performance of comparative assessment of the impact of surfacing technique and technology, as well as surfacing materials, on the fatigue life of specimens. 17 Ref., 3 Tables, 9 Figures.

Keywords: arc surfacing, manufacturing surfacing, repair surfacing, fatigue, fatigue life, fatigue cracks, stress intensity factor

In metallurgy and mechanical engineering, tools and equipment for hot deformation of metals and alloys are widely used, which are exposed to cyclic mechanical and thermal loads during service. The examples of such heavy-loaded parts are different mill rolls, MCCB rollers, etc. Therefore, the problem of evaluation of fatigue life of such parts becomes particularly acute when it is necessary to evaluate the parts restored by different methods, including the methods of electric arc surfacing. [1–5].

Such parts have already passed a certain period of service and have exhausted a part of their life, specified during their designing and manufacture. After a series of subsequent repairs by surfacing methods, as a result of a nonuniform temperature distribution along the cross-section of a part, unfavorable residual tensile stresses are often formed in it [6–8]. In addition, the more times it was subjected to repairs and, accordingly, a bigger number of deposited layers it has the higher the probability of defects in the deposited metal in the form of lacks of fusion, slags, pores, etc. [4–10].

The most dangerous zones of mill rolls, in which cracks may appear, are the central areas, displaced from the axis of the roll towards variable total stresses having non-zero amplitude [5]. Also, an increased probability of crack formation and their higher growth rate are resulted by a decrease in the coefficient of asymmetry of the cycle and a significant range of the stress intensity factor (SIF) in the zone of the edge effect [5].

During service, all these factors negatively affect the overall fatigue life, which can lead to appearance and propagation of mechanical and fatigue cracks and, as a consequence, to the emergency fracture of parts.

Therefore, when developing the technology of repair surfacing of such parts, it is necessary to carefully evaluate the impact of preliminary service, chemical composition and properties of surfacing materials, as well as technological parameters of the arc surfacing process on the residual life of a restored part.

The aim of the work is to establish the fatigue life of the deposited specimens after manufacturing and repair surfacing, as well as to evaluate the impact of

I.O. Ryabtsev — <https://orcid.org/0000-0001-7180-7782>, V.V. Knysh — <https://orcid.org/0000-0003-1289-4462>

A.A. Babinets — <https://orcid.org/0000-0003-4432-8879>, S.O. Solovej — <https://orcid.org/0000-0002-1126-5536>

V.M. Demenkov — <https://orcid.org/0000-0002-2000-0783>

© I.O. Ryabtsev, V.V. Knysh, A.A. Babinets, S.O. Solovej and V.M. Demenkov, 2020

Table 1. Chemical composition of base and deposited metals, wt.% [11]

Grade of steel	C	Mn	Si	Cr	V	Mo	S	P
40Kh	0.36–0.40	0.5–0.8	0.17–0.37	0.8–1.1	–	–	≤0.035	≤0.035
PP-Np-25Kh5FMS*	0.20–0.32	0.5–1.0	0.80–1.30	4.6–5.8	0.2–0.6	0.9–1.5	≤0.04	≤0.04
4Kh5MFS**	0.32–0.40	0.2–0.5	0.90–1.20	4.5–5.5	0.3–0.5	1.2–1.5	≤0.04	≤0.04

Table 2. Mechanical properties of base and deposited metals [11]

Grade of steel	Mechanical properties (after normalization)					
	Conditional yield strength $\sigma_{0.2}$, MPa	Tensile strength σ_t , MPa	Relative elongation after rupture δ , %	Relative reduction in area after rupture ψ , %	Impact toughness KCU , J/cm ² , for specimens at $t = 20$ °C	Hardness
40Kh	345	590	12.5	52	7.5	HB 174–217
4Kh5MFS**	1570	1710	12	54	51	HRC 48–50

Notes to Tables 1 and 2:

*Presented mass fraction of elements in the deposited metal.

**In the literature there is no data on mechanical properties of metal deposited by the wire PP-Np-25Kh5FMS. Therefore, the data are presented for its analogue, which as to its chemical composition and properties is the closest to steel 4Kh5MFS.

the developed technology of repair surfacing on the overall life of a part.

Materials and methods of investigations. The choice of the type of base and deposited metal was grounded on the analysis of data from the technical literature: as the base metal in mill rolls, usually medium- and high-carbon non-alloyed or low-alloyed structural steels of such grades as 45, 50, 40 Kh, 50 Kh, 50KhN etc. are used. For surfacing of the working wear-resistant layer of mill rolls and other similar parts, electrode materials are most often used, such as heat-resistant or semi-heat-resistant steels, which provide producing a deposited layer. Such materials include flux-cored wires of grades PP-Np-25Kh5FMS, PP-Np-35V9Kh3SF, PP-Np-30Kh4V2M2FS, etc. [1, 3, 5].

Based on these data, for investigations as the base metal, steel 40Kh was chosen in the work. For surfacing the working layer, the flux-cored wire PP-Np-25Kh5FMS was used, which is widely applied in surfacing of mill rolls [8]. The chemical composition and mechanical properties of the materials used in the work are given in Tables 1 and 2.

At present, there is no single standardized procedure for fatigue tests of multilayer deposited specimens aimed at establishing their cyclic fatigue life. Most researchers use their own developed procedures that simulate the shape and features of specific parts the best [6, 10, 12, 13]. Taking into account a wide variety of parts operated under conditions of fatigue loading, such approach provides more reliable results. However, the abovementioned procedures do not allow evaluating the influence of surfacing materials and geometric dimensions of deposited specimens on their fatigue life. The authors [14, 15] proposed a procedure that allows correcting these drawbacks and can be successfully used for comparative evaluation of fatigue life of deposited parts, clearly demonstrat-

ing the influence of chemical composition of surfacing materials, deposited layers and surfacing scheme on the cyclic fatigue life of specimens.

The shape and dimensions of the deposited specimens for fatigue tests, the technology of their manufacture, as well as the testing procedure itself were chosen based on the calculations, recommendations and results of preliminary tests, which are given in [14, 15]. The tests according to this procedure reproduce the force loads, typical for mill rolls with a certain assumption, and in the course of tests allow carrying out a visual evaluation of the rate of fatigue crack propagation.

Taking into account the fact, that the authors of this work planned to carry out comprehensive investigations of fatigue life of parts deposited by different technologies using different materials of the main and intermediate layers. Therefore, to carry out a comparative evaluation of fatigue life of specimens after manufacturing and repair surfacing the developed procedure [14, 15] was used, having the improvements described below.

According to the surfacing technology described in [14, 15], 3 series of specimens were manufactured, 3 specimens in each series.

The first series of specimens was tested for fatigue until their complete fracture. The fatigue investigations were performed in the test servohydraulic machine URS-20 at three-point bending with a cycle asymmetry $R_\sigma = 0$ and a frequency of 5 Hz at a regular loading. The maximum stresses of the cycle were 500 MPa, and the distance between the supports was 250 mm.

On the second series of specimens cyclic crack resistance was evaluated. To initiate the propagation of a fatigue crack in the deposited metal in the center of the specimen (in the area of maximum applied stresses) a V-shaped notch with a depth of 1.0–1.5 mm with a radius of 0.25 mm was performed. After that, at a three-point cyclic bending with the maximum level of

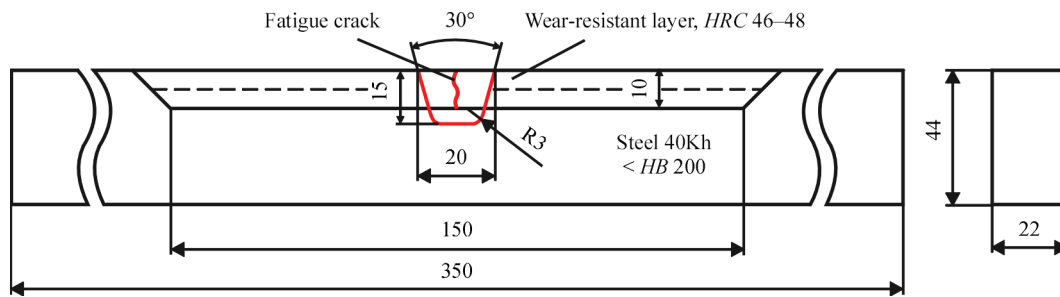


Figure 1. Scheme of preparation of metal damaged by fatigue cracks

applied stresses in the cross-section of the specimen of 300 MPa, a fatigue crack was grown until a length of 1 mm on one of the side faces. As a result, the produced notch with a crack was taken as the initial fatigue crack in the test specimen, which was then used to study the kinetics of fatigue fracture. When conducting fatigue tests for cyclic crack resistance, the length of a fatigue crack, which propagated on the side face of the specimen, was measured using an optical microscope with a graduating mark of 0.01 mm. The tests were performed until a complete fracture of the specimens.

In addition, for the specimens applying the numerical method based on the finite-element method (FEM), the stress-strain state was determined and the SIF was calculated on the crack front. The SIF is the main parameter of crack resistance and represents a quantitative evaluation of the stress field at the stage of arising fracture near the crack tip. The stress field at the crack tip has a singularity of the form $1/\sqrt{r}$, where r is the distance from the crack tip to the point where stresses are considered [16].

Determination of these characteristics for specimens made applying the abovementioned technology, and for the specimens made later by other technologies, will allow carrying out a comparative evaluation of their cyclic crack resistance, where the values obtained in this work will act as basic values.

On the specimens of the third series the efficiency of repair surfacing was investigated to increase the residual cyclic fatigue life of specimens, having fatigue cracks in the deposited wear-resistant layer. The specimens were tested for fatigue at a three-point bending with the asymmetry of the cycle $R_\sigma = 0$ until the formation of a fatigue crack with a depth of 10–12 mm (when the crack passed through the deposited layers and deepened into the base metal) (Figure 1). After that, repair was carried out applying arc surfacing methods, which consisted of a complete mechanical removal of a fatigue crack, the metal around it and the subsequent filling of the formed groove (Figure 2).

The depth and width of the groove, as well as the lateral radii were selected according to the maximum length of fatigue cracks, as well as according to practical recommendations to produce a quality deposited joint under the flux layer for the corresponding metal thickness. The development of such sizes and shape allows preventing jamming of the slag crust, which could result in the formation of slags, which, in turn,

can reduce mechanical properties of the deposited metal, acting as stress concentrators.

After mechanical treatment, the specimens with a groove for repair surfacing (Figure 2, *a*) were collected in a package (3 pcs), laying by two technological inserts between the specimens with a thickness of 3 mm each. From both free edges, to the specimens run-on plates were attached (Figure 2, *b*).

Before surfacing, preliminary heating of packages of billets to 250–300 °C was carried out. After that, automatic arc surfacing of the wear-resistant layer was performed using the flux-cored wire PP-Np-25Kh5FMS with a diameter of 1.8 mm under the flux AN-26P.

The surfacing mode for all the specimens was the same: $I = 220\text{--}250$ A; $U = 26\text{--}28$ V; $v = 18$ m/h; overlap of the beads ≈ 50 %. After surfacing, the speci-

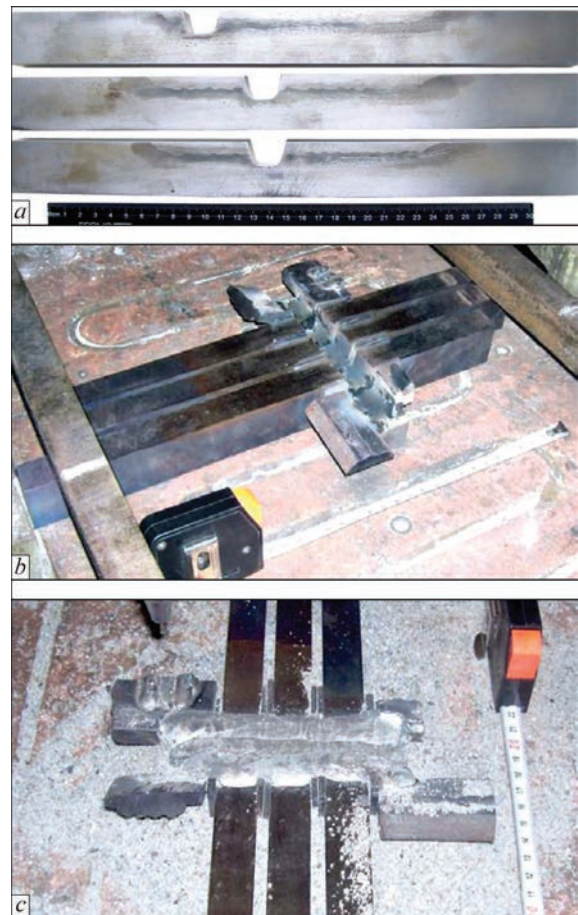


Figure 2. Appearance of billets with preparation for repair surfacing (*a*), assembled into a package before (*b*) and after repair surfacing (*c*)

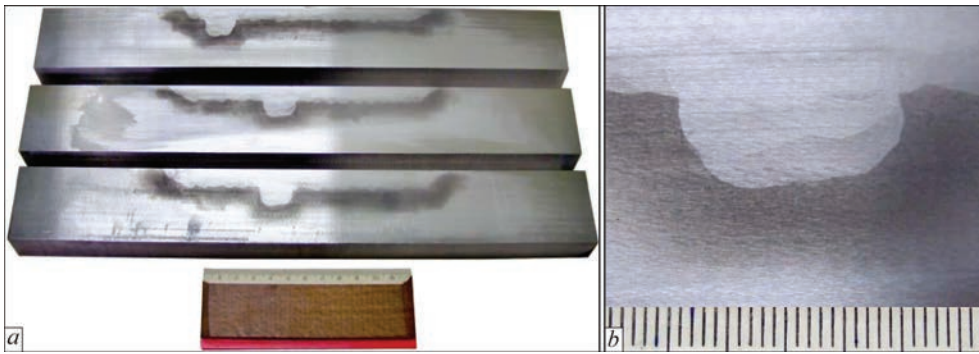


Figure 3. Appearance of specimens after grinding (a) and area of repair surfacing (b)

mens were placed in a thermal oven heated to 250 °C for slow cooling together with it. Such measures were aimed at reducing residual stresses in the deposited specimens and the probability of cracking.

After a complete cooling, the package of repaired specimens was cut with the help of abrasive discs on technological inserts into separate specimens, which were finally treated by grinding on four sides (Figure 3) and again were installed in the test machine.

Before the fatigue test, in the specimens repaired by surfacing, residual stresses were measured by the nondestructive acoustic method using a portable ultrasonic stress control device [17]. Ultrasonic quartz sensors of longitudinal and shear waves with a measurement base of 7×7 mm were used.

Discussion of results. The fatigue tests of the first series of specimens showed that their cyclic fatigue life before fracture at maximum applied stresses of 500 MPa is in the range from 560800 to 1420100 cycles of stress changes.

A preliminary visual inspection of the specimens with ×10 magnification showed that fatigue cracks mainly appear near the fusion zone of two adjacent beads, which can be explained by an increase in the level of chemical and structural heterogeneity in that zone [5]. In this case, a crack usually propagates almost rectilinearly, parallel to the direction of the applied load with small lateral branches. Moreover, it is

noted that in the «channel» of the crack some bends and short tears are observed (Figure 4). Subsequently, the areas of metal with fatigue cracks were cut out and microsections were made. The investigations of microsections showed that fatigue cracks are mainly formed and propagated near the zones of overlaps of adjacent deposited beads, propagating in the direction of the axes of dendrites formation (Figure 5).

Therefore, it was found that the type and the nature of formation and further propagation of fatigue cracks depends on the technique and technology of surfacing, in particular, on the step during surfacing of adjacent beads. Moreover, the fusion line of the base and deposited metals, as well as the nature of the fusion line of separate beads and layers play an important role in the process of fatigue fracture of deposited parts, because cracks mostly propagate either along the fusion boundary of separate beads, or directly near this boundary, where the zone of chemical and structural heterogeneity is probably located, which negatively affects the fatigue life.

On the specimens of the second series during experimental investigations of crack resistance, the dependence of fatigue crack (depth) propagation on the corresponding number of cycles of variable load N was determined. After initiation, all fatigue cracks propagated as non-through (corner) ones from one of the edges of the specimen. Therefore, in addition to the crack depth along the vertical side face of the spec-

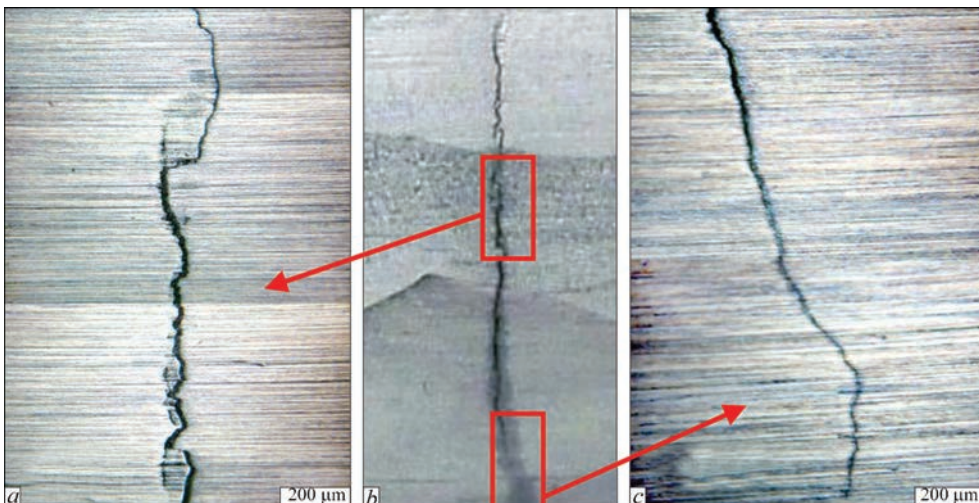


Figure 4. Nature of propagation of fatigue cracks in deposited specimens

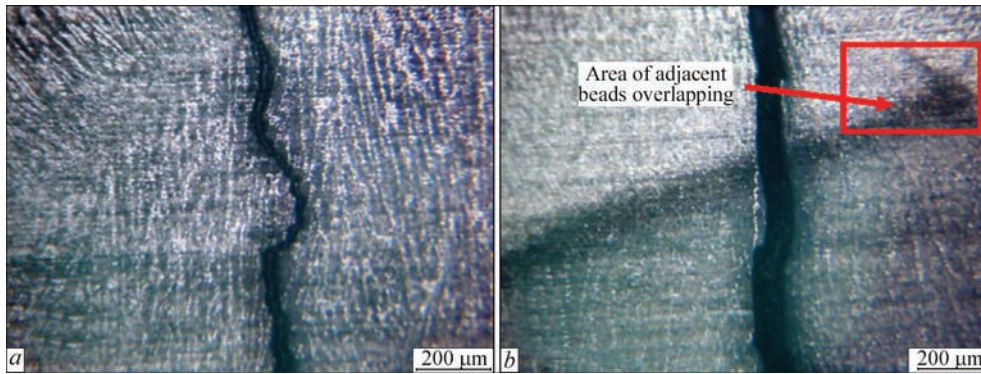


Figure 5. Nature of propagation of fatigue cracks in deposited metal. Magnification $\times 50$

imen, the crack length at the bottom of the V-shaped notch was also measured using a caliper with a graduating mark of 0.1 mm. The fracture of the specimens during three-point cyclic bending with a maximum level of applied stresses of 300 MPa occurred when the cracks reached the dimensions (depth \times length): 23.6 \times 16.4, 12 \times 14 and 14 \times 16 mm.

Using numerical method based on FEM, the stress-strain state (Figure 6) was determined and calculation of SIF along the crack front (Figure 7) was carried out. Figure 6 shows the stress-strain state in the model specimen at the beginning of fatigue fracture (crack size of 6 \times 4 mm, Figure 6, *a*) and when the crack reaches its critical value 23.6 \times 16.4 (Figure 6, *b*).

Figure 7 shows the data of change in SIF values along the crack front (zero value on the abscissa axis corresponds to the beginning of the crack on the vertical side face of the specimen) as the corner crack propagates in the two specimens of the second series. The construction of a finite-element model of the specimen and the subsequent SIF calculations were performed by means of the software package ANSYS Workbench 2019R3. The calculation CE-grid consisted of 20 nodal hexagonal elements and of 15 nodal prismatic elements directly along the crack front. In the area of the crack front, a grid with a concentric arrangement of elements was built, which consisted of 16 layers of elements in the radial and 48 layers in the circumferential directions, which uniformly surrounded the crack front. This

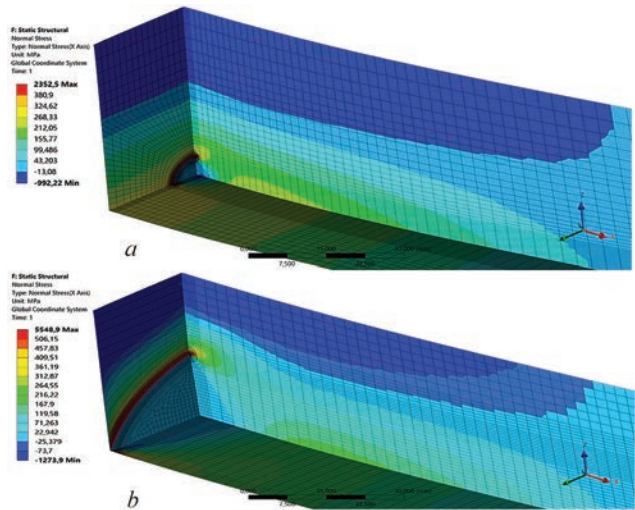


Figure 6. Results of calculation of stress-strain state for cracks with the sizes of 6 \times 4 (*a*) and 23.6 \times 16.4 mm (*b*)

allowed solving the problem of fracture mechanics with the required accuracy.

It was established that the maximum values of SIF along the crack front are at a distance of about 1 mm from the vertical side face at the deepest point of the crack front and during fracture they reach the value of 52–64 MPa \sqrt{m} .

On the specimens of the third series, after performing repair surfacing, residual stresses were measured by nondestructive ultrasonic method using the de-

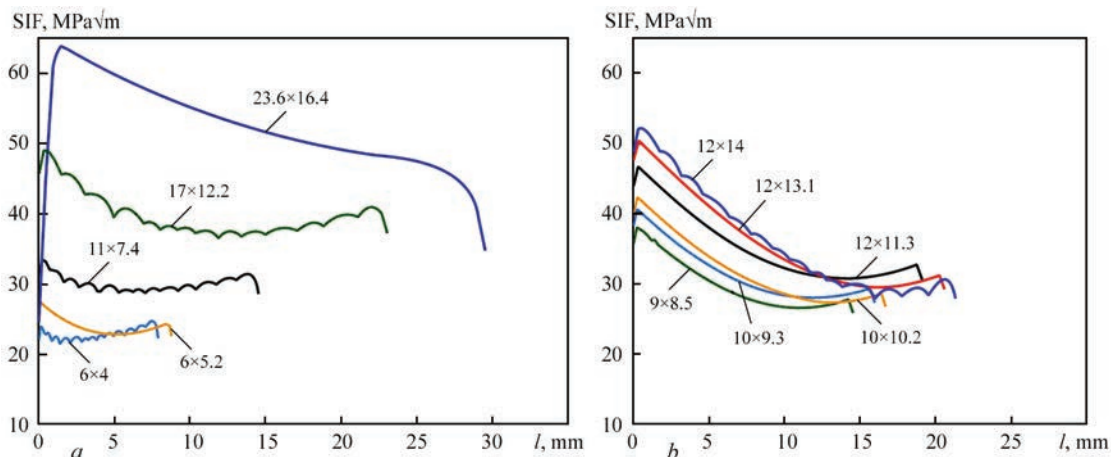


Figure 7. Values of SIF on the crack front as it propagates in the first (*a*) and the second (*b*) specimens of the second series

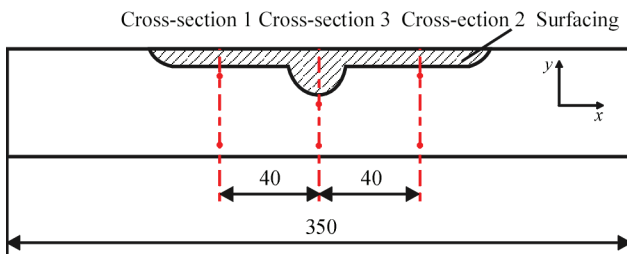


Figure 8. Schematic representation of places of measuring residual stresses in the specimen after repair surfacing

veloped technology. Schematic representation of the places of measurement of residual stresses is given in Figure 8, and diagrams of the distribution of residual stresses are in Figure 9. The measurements of residual stresses oriented along and across the specimen were performed from the fusion line (determined by the macrostructure) deep into the metal. The values of residual stresses given on the diagrams are averaged over the thickness of the specimen.

The use of ultrasonic quartz sensors of longitudinal and shear waves with a measurement base of 7×7 mm did not allow performing the measurement of stresses closer than 2.5 mm to the fusion line. However, the study of residual fields σ_x oriented along the specimen (coincide in direction with the applied operating stresses during tests of the specimens on fatigue) showed that the zone of residual tensile stresses after repair surfacing does not exceed 6–7 mm from the fusion line deep into the base metal. The maximum residual tensile stresses σ_x are located directly in the area of repair surfacing and amount to about 120 MPa at a distance of 2.5 mm from the fusion line (Figure 9, *b*). In the course of moving away from the place of

repair surfacing, the residual tensile stresses σ_x at a distance of 2.5 mm from the fusion line are reduced to 40–80 MPa (Figure 9, *a, c*). Starting from a distance of 6–7 mm from the fusion line deep into the metal, a zone of residual compressive stresses is formed, which reach the values of up to –60––80 MPa. These data will also be used as a basis for further comparative investigations of fatigue life of specimens deposited by other technologies.

After measuring the residual stresses, the specimens of the third series were subjected to fatigue tests. The results of fatigue tests of specimens of the third series before and after repair surfacing are given in Table 3.

A preliminary fatigue crack initiation in the specimen No.8 (Table 3) occurred inside the specimen at a distance of 8 mm from the surface (near the fusion line with the base metal) as a result of a lack of fusion between the beads. At the same time, elimination of fatigue cracks by repair surfacing, the occurrence of which is caused by casual technological defects in a preliminary deposited layer, does not lead to a decrease in life as compared to defect-free surfacing. After repair surfacing, the initiation and propagation of fatigue cracks in all specimens of the third series took place at a far distance from the place of repair. Fatigue tests of the specimens of the third series showed that a total cyclic fatigue life of the specimens at maximum applied stresses of 500 MPa is in the range from 1154000 to 1651700 cycles of stress changes.

It is also shown (specimen No.9, Table 3) that application of repair surfacing to the products with fatigue cracks after their long service does not lead to a significant increase in cyclic fatigue life after repair.

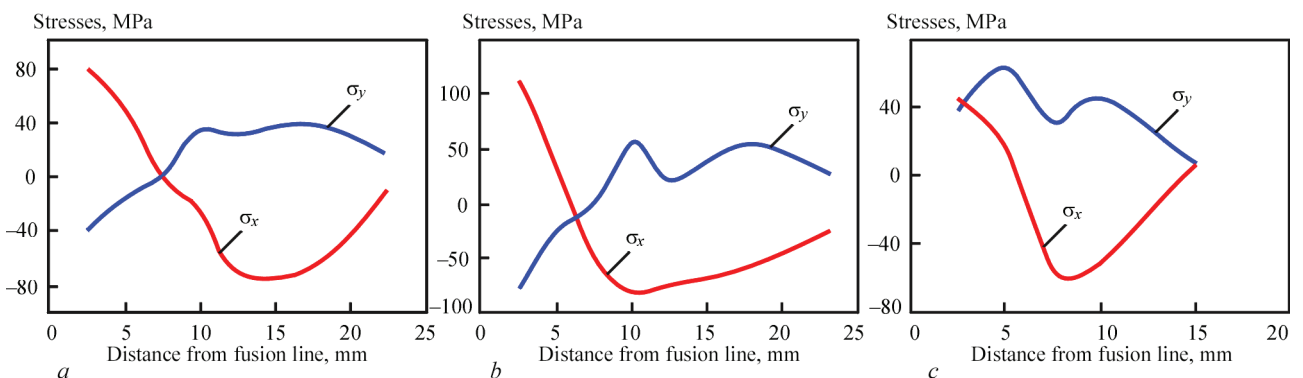


Figure 9. Distribution of residual stresses oriented along σ_x and across σ_y of the specimen after repair surfacing in the cross-section 1 (*a*), cross-section 2 (*b*) and cross-section 3 (*c*)

Table 3. Results of fatigue tests of specimens of the third series

Number of specimen	Maximum cycle stresses, MPa	Cyclic fatigue life before formation of a crack of 10 mm, cycles	Cyclic fatigue life after repair surfacing, cycles	Total cyclic fatigue life, cycles
7	500	688700	963000	1651700
8	500	132800*	1021200	1154000
9	500	1381800	128000	1509800

*Defect in the form of lack of fusion between the beads.

This is associated with the fact that after long-term service, the defect-free layer of deposited metal has a significant level of accumulated fatigue damages and that is the reason why repairing of the area of a product damaged by a fatigue crack is inefficient without a complete removal of the deposited metal layer. Therefore, repairing products after long-term service in order to significantly increase the overall life, it is recommended to remove not only the metal around the revealed fatigue cracks, but the whole deposited layer to the depth of the revealed fatigue cracks with a subsequent restoration surfacing.

Conclusions

1. Design of the deposited specimens and procedure of comparative investigations of their fatigue life were improved, as well as the basic fatigue characteristics of the deposited specimen, simulating the design of mill rolls, were established.

2. It was established that the type and the nature of formation and further propagation of fatigue cracks in the deposited specimens depend on the technique and technology of surfacing, in particular, on the step during surfacing of adjacent beads. In addition, the fusion line of the base and deposited metals, as well as the nature of the fusion line of particular beads and layers plays an important role in the process of fatigue fracture of deposited parts, because cracks mostly propagate either along the fusion boundary of separate beads, or directly near this boundary, where, probably, the zone of chemical and structural heterogeneity is located, which negatively affects the fatigue life.

3. Using the numerical method based on FEM, the SIF values were determined along the front of the non-through corner fatigue crack, which propagated in a prismatic model specimen of 40Kh steel with a wear-resistant deposited metal layer at a three-point repeating cyclic bending. It was established that the maximum values of SIF along the crack front are located at a distance of about 1 mm from the vertical side face at the deepest point of the crack front and during fracture they reach the value of 52–64 MPa \sqrt{m} .

4. It was experimentally established that at the early stages of service of a product the elimination of fatigue cracks by repair surfacing, the appearance of which is caused by random technological defects in the preliminary deposited layer, does not lead to a decrease in the life as compared to defect-free surfacing.

5. It was shown that application of repair surfacing to the products with fatigue cracks after their long-term service does not lead to a significant increase in the cyclic fatigue life after repair. This is associated with the fact that after long-term service, the defect-free layer of deposited metal has a significant level of accumulated fatigue damages. Therefore, the repair of a product damaged by a fatigue crack with-

out a complete removal of the deposited metal layer is not effective enough.

- Gao, F., Zhou, J., Zhou, J. et al. (2017) Microstructure and properties of surfacing layers of dies manufactured by bi-metal-gradient-layer surfacing technology before and after service. *The Int. J. Adv. Manuf. Technol.*, **88**, 1289–1297. doi:10.1007/s00170-016-8679-0
- Zhang, J., Zhou, J., Tao, Y. et al. (2015) The microstructure and properties change of dies manufactured by bimetal-gradient-layer surfacing technology. *Ibid.*, **80**, 1807–1814. doi:10.1007/s00170-015-7170-7
- Ahn, D.-G. (2013) Hardfacing technologies for improvement of wear characteristics of hot working tools: A review. *Int. J. of Precision Engineering and Manufacturing*, **14**(7), 1271–1283. doi:10.1007/s12541-013-0174-z
- Jhavar, S., Paul, C.P., Jain, N.K. (2013) Causes of failure and repairing options for dies and molds: A review. *Engineering Failure Analysis*, **34**, 519–535. DOI: 10.1016/j.engfailanal.2013.09.006
- Du, Toit, M., Van, Niekerk J. (2010) Improving the life of continuous casting rolls through submerged arc cladding with nitrogen-alloyed martensitic stainless steel. *Welding in the World*, **54**(11–12), 342–349. doi:10.1007/bf03266748
- Shao, C., Cui, H., Lu, F., Li, Z. (2019) Quantitative relationship between weld defect characteristic and fatigue crack initiation life for high-cycle fatigue property. *Int. J. of Fatigue*, **123**, 238–247. doi:10.1016/j.ijfatigue.2019.02.028
- Korotkov, V.A. (2017) More efficient surfacing. *Russian Engineering Research*, **37**, 701–703. doi:10.3103/S1068798X17080093
- Rjabcev, I.A., Senchenkov, I.K., Turyk, Je.V. (2015) *Surfacing. Materials, technologies, mathematical modeling*. Gliwice, Wydawnictwo politechniki slaskiej [in Russian].
- Liu, H., Yang, S., Xie, C. et al. (2018) Mechanisms of fatigue crack initiation and propagation in 6005A CMT welded joint. *J. of Alloys and Compounds*, **741**, 188–196. doi:10.1016/j.jallcom.2017.12.374
- Zerbst, U., Madia, M., Beier, H. T. (2017) Fatigue strength and life determination of weldments based on fracture mechanics. *Procedia Structural Integrity*, **7**, 407–414. doi:10.1016/j.prostr.2017.11.106
- Oberg, E. et al. (1996) *Machinery's Handbook* (25th ed.), Industrial Press Inc.
- Zhang, D., Liu, Y., Yin, Y. (2016) Preparation of plasma cladding gradient wear-resistant layer and study on its impact fatigue properties. *J. Thermal Spray Technol.*, **25**, 535–545. doi:10.1007/s11666-015-0370-8
- Ganesh, P., Moitra, A., Tiwari, P. et al. (2010) Fracture behavior of laser-clad joint of Stellite 21 on AISI 316L stainless steel. *Mater. Sci. & Engin.*, **527** (16–17), 3748–3756. doi:10.1016/j.msea.2010.03.017
- Babinets, A.A., Ryabtsev, I.A. (2016) Fatigue life of multi-layer hard-faced specimens. *Welding Int.*, **30**(4), 305–309. <https://doi.org/10.1080/01431161.2015.1058004>
- Ryabtsev, I.A., Knysh, V.V., Babinets, A.A. et al. (2019) Methods and specimens for comparative investigations of fatigue resistance of parts with multilayer surfacing. *The Paton Welding J.*, **2**, 29–34. <https://doi.org/10.15407/tpwj2019.02.05>
- Murakami, Yu. (1990) *Reference book on stress intensity coefficients*. In: 2 Vol. Moscow, Mir [in Russian].
- (2004) *Device for control of mechanical stresses and strains in solid media*. Pat. UA 71637 C2 [in Ukrainian].

Received 24.07.2020